

NLRC3, a Member of the NLR Family of Proteins, Is a Negative Regulator of Innate Immune Signaling Induced by the DNA Sensor STING

Lu Zhang,^{1,2} Jinyao Mo,³ Karen V. Swanson,¹ Haitao Wen,¹ Alex Petrucelli,¹ Sean M. Gregory,¹ Zhigang Zhang,¹ Monika Schneider,⁴ Yan Jiang,⁶ Katherine A. Fitzgerald,⁷ Songying Ouyang,⁶ Zhi-Jie Liu,⁸ Blossom Damania,^{1,4} Hong-Bing Shu,⁹ Joseph A. Duncan,³ and Jenny P.-Y. Ting^{1,4,5,*}

¹Lineberger Comprehensive Cancer Center

²Department of Oral Biology, School of Dentistry

³Department of Medicine, Division of Infectious Diseases

⁴Department of Microbiology and Immunology

⁵Institute of Inflammatory Diseases and Center for Translational Immunology

University of North Carolina at Chapel Hill, Chapel Hill, NC 27599, USA

⁶National Laboratory of Biomacromolecules, Institute of Biophysics, Chinese Academy of Sciences, Beijing 100101, China

⁷Division of Infectious Disease and Immunology, Department of Medicine, University of Massachusetts Medical School, Worcester, MA 01605, USA

⁸iHuman Institute, ShanghaiTech University, Shanghai 201210, China

⁹State Key Laboratory of Virology, College of Life Sciences, Wuhan University, Wuhan 430072, China

*Correspondence: jenny_ting@med.unc.edu

<http://dx.doi.org/10.1016/j.immuni.2014.01.010>

SUMMARY

Stimulator of interferon genes (STING, also named MITA, MYPS, or ERIS) is an intracellular DNA sensor that induces type I interferon through its interaction with TANK-binding kinase 1 (TBK1). Here we found that the nucleotide-binding, leucine-rich-repeat-containing protein, NLRC3, reduced STING-dependent innate immune activation in response to cytosolic DNA, cyclic di-GMP (c-di-GMP), and DNA viruses. NLRC3 associated with both STING and TBK1 and impeded STING-TBK1 interaction and downstream type I interferon production. By using purified recombinant proteins, we found NLRC3 to interact directly with STING. Furthermore, NLRC3 prevented proper trafficking of STING to perinuclear and punctated region, known to be important for its activation. In animals, herpes simplex virus 1 (HSV-1)-infected *Nlrc3*^{-/-} mice exhibited enhanced innate immunity and reduced morbidity and viral load. This demonstrates the intersection of two key pathways of innate immune regulation, NLR and STING, to fine tune host response to intracellular DNA, DNA virus, and c-di-GMP.

INTRODUCTION

Nucleic acid and small nucleic acid-like molecules can act as pathogen-associated molecular patterns (PAMPs) to cause type I interferon (IFN-I) and other cytokine induction (Takeuchi and Akira, 2007). Among DNA sensors, STING (also referred to

as mediator of IRF3 activation [MITA], plasma membrane tetra-spanner [MPYS], or endoplasmic reticulum IFN stimulator [ERIS]) has emerged as central for DNA-induced IFN-I activation (Ishikawa et al., 2009; Jin et al., 2008; Sun et al., 2009; Zhong et al., 2008). Other DNA sensors such as gamma-interferon-inducible protein16 (IFI16) and DEAD (Asp-Glu-Ala-Asp) box polypeptide 41 (DDX41) are known to activate IFN-I in a STING-dependent manner (Unterholzner et al., 2010; Zhang et al., 2011).

The nucleotide binding domain (NBD) and leucine-rich-repeat (LRR) containing proteins (NLRs) are intracellular sensors that regulate inflammatory responses (Eisenbarth and Flavell, 2009; Shaw et al., 2010). Most NLRs positively influence inflammatory responses, particularly the inflammasome NLRs. However, emerging studies of gene-deficient mice have revealed that several NLRs negatively affect innate immune responses (Allen et al., 2011, 2012; Anand et al., 2012; Cui et al., 2010; Schneider et al., 2012; Xia et al., 2011; Zaki et al., 2011). Notably, we have previously shown that a caspase activating and recruitment domain (CARD)-containing NLR, NLRC3, reduces LPS-induced nuclear factor kappa B (NF- κ B) activation through inhibiting the adaptor protein TNF receptor associated factor 6 (TRAF6) (Schneider et al., 2012). However, the intersection of NLRs with DNA-sensing molecules has not been described. In this report, we find that NLRC3 deficiency also leads to increased innate immune response to intracellular DNA and c-di-GMP in both hematopoietic and nonhematopoietic cells. NLRC3 interacts with STING and the protein kinase TBK1, leading to reduced STING-TBK1 association, improper STING trafficking, and decreased activation of innate immune cytokines. However, this interference is separate from the previously described function of NLRC3 in impeding TRAF6 activation during LPS response. This work reveals the intersection of NLR with

STING-mediated DNA sensing and unveils the multifacet function of the NLR family.

RESULTS

NLRC3 Deficiency Leads to Elevated DNA- and HSV-1-Induced IFN-I and Cytokine Production

During our screening of NLR-deficient cells for new functions, we observed that IFN-I protein (Figure 1A) was higher in *Nlrc3*^{-/-} bone-marrow-derived macrophages (BMDMs) than in those of wild-type (WT) cells. This enhancement was observed in response to transfected poly(dA:dT) but not to extracellular poly(dA:dT), poly(I:C), or LPS (Figure 1A). Interleukin-6 (IL-6) protein was also higher in *Nlrc3*^{-/-} BMDMs in the presence of intracellular poly(dA:dT) but not extracellular poly(dA:dT) (Figure 1B). In addition, the effect of NLRC3 was extended to the interferon stimulatory DNA (ISD), which has been used to more specifically demonstrate cytoplasmic DNA sensing (Chiu et al., 2009; Stetson and Medzhitov, 2006). NLRC3 also negatively regulates IFN-I (Figures 1C–1E) and IL-6 (Figure S1A available online) responses to ISD in mouse embryonic fibroblasts (MEFs). These results suggest that NLRC3 functions as a negative regulator of cytoplasmic DNA sensing. To determine its role in a more physiologic setting, *Ifna4* and *Ifnb* response to a DNA virus, Herpes simplex virus 1 (HSV-1), was tested and found to be higher in *Nlrc3*^{-/-} BMDMs (Figures 1F and 1G) and peritoneal macrophages (Figures 1H and 1I). The impact of NLRC3 is not limited to type I IFN because tumor necrosis factor (TNF) protein and transcript were similarly increased (Figures 1J and 1K). However, NLRC3 did not affect various responses to the Sendai RNA virus (SeV) (Figure 1K).

To assess whether the suppressive role of NLRC3 on DNA-induced IFN-I and cytokine response is exhibited in nonimmune cells, pairs of *Nlrc3*^{+/+} and *Nlrc3*^{-/-} MEFs were isolated from siblings from heterozygous matings. *Ifnb* and *Tnf* transcripts were significantly increased in *Nlrc3*^{-/-} MEFs in response to HSV-1 (Figures 1L and 1M), as were IFN- β and IL-6 proteins (Figures 1N and 1O). However, *Nlrc3*^{-/-} MEFs responded normally to SeV (Figure 1O). The lack of an effect of NLRC3 on poly(I:C) or RNA virus-induced cytokine responses was more extensively analyzed. Wild-type and *Nlrc3*^{-/-} cells responded similarly to Sendai virus, intracellular or extracellular poly(I:C), and vesicular stomatitis virus (VSV) under a variety of test conditions (Figure S2).

Because of concerns about variations in MEFs, we isolated a second pair of sibling-matched MEFs, and identical effects of *Nlrc3* deletion on *Ifna4* and *Ifnb* transcripts was observed, indicating that the suppressive effect of NLRC3 was not due to artificial differences in one specific pair of gene-sufficient and -deficient MEFs (Figures S1B–S1D). Similar results were observed when IFN- β protein was measured. Consistent with increased cytokines, which would be expected to reduce viral load, HSV-1 genomic DNA copy number was significantly reduced in *Nlrc3*^{-/-} MEFs (Figure 1P) and BMDMs (Figure 1Q). However, HSV-1-mediated cell death was not altered in *Nlrc3*^{-/-} MEFs, indicating that the observed differences were not due to different cell viability (Figure S3). These data demonstrate that NLRC3 attenuates cytokine response to intracellular DNA without affecting cell viability.

NLRC3 Deficiency Causes Increased IFN- β and IL-6 Production in Response to c-di-GMP and c-di-GMP

c-di-GMP, a small dinucleotide monophosphate, is a second messenger of bacteria such as *Listeria monocytogenes* and *Burkholderia thailandensis* and activates the IFN-I response via interaction with STING (Burdette et al., 2011; Jin et al., 2011; Sauer et al., 2011). *Nlrc3*^{-/-} MEFs produced more IFN- β and IL-6 proteins in response to transfected c-di-GMP (Figures 2A and 2B). Additionally, *Nlrc3*^{-/-} MEFs produced increased IFN-I and IL-6 in response to infection with c-di-GMP-producing *L. monocytogenes* (Figures 2C–2E). Increased IFN- β was also observed in *Nlrc3*^{-/-} cells infected with another c-di-GMP-producing bacteria, *B. thailandensis* (Figure 2F). Thus, *Nlrc3* deficiency leads to increased innate immune response to cytoplasmic DNA, c-di-GMP, and bacteria that produce c-di-GMP.

NLRC3 Inhibits the STING-Dependent Pathway

Cytoplasmic DNA and c-di-GMP induce IFN-I through the STING molecule, which led us to examine both functional and molecular interactions between NLRC3 and STING (Burdette et al., 2011; Huang et al., 2012; Ouyang et al., 2012; Shang et al., 2012; Shu et al., 2012). To investigate whether NLRC3 affects the STING pathway, we examined the impact of NLRC3 on the activation of IFN- β promoter-luciferase by STING. This reporter assay was internally controlled by the cotransfection of a Renilla luciferase construct. NLRC3 inhibited IFN- β promoter activation by STING by 9.72-fold. STING operates by interaction and activation of its downstream kinase, TBK1 (Tanaka and Chen, 2012). NLRC3 dramatically reduced IFN- β promoter activation by TBK1. However, NLRC3 had no direct effect on the downstream interferon regulatory transcription factor 3 (IRF3), indicating that NLRC3 probably functions at the upstream STING-TBK level (Figure 3A). As a specificity control, another NLR, NLRP11, did not reduce IFN- β promoter activation by TBK1 (Figure 3B). NLRC3 also inhibited a second promoter driven by the canonical interferon-stimulated responsive element (ISRE), which is known to be activated by STING and TBK1 (Figure 3C; Ishikawa and Barber, 2008; Zhong et al., 2008). However, NLRC3 had no effect on the activation of the ISRE promoter by mitochondrial antiviral signaling protein (MAVS) (also referred to as interferon-beta promoter stimulator 1 [IPS-1], virus-induced signaling adaptor [VISA], and CARD adaptor inducing IFN- β [CARDIF]), which is important for RNA sensing, nor did it affect promoter activation by the downstream IRF3 (Figure 3C). In addition, NLRC3 inhibited NF- κ B promoter activated by STING and reduced MAVS activation slightly but did not affect retinoic acid-inducible gene 1 (RIG-I) (Figure 3D). We also observed that NLRC3 inhibited c-di-GMP and poly(dA:dT)-induced ISRE activation (Figure 3E). These experiments indicate that the predominant effect of NLRC3 is on the STING pathway. As an additional specificity control for NLR proteins, overexpression of NLRC5, which has been reported to inhibit various innate immune pathways when tested in an overexpression system (Cui et al., 2010), did not inhibit STING- or TBK1-induced ISRE activation (Figure 3F). These experiments suggest that NLRC3 downregulates innate immunity caused by STING and TBK1.

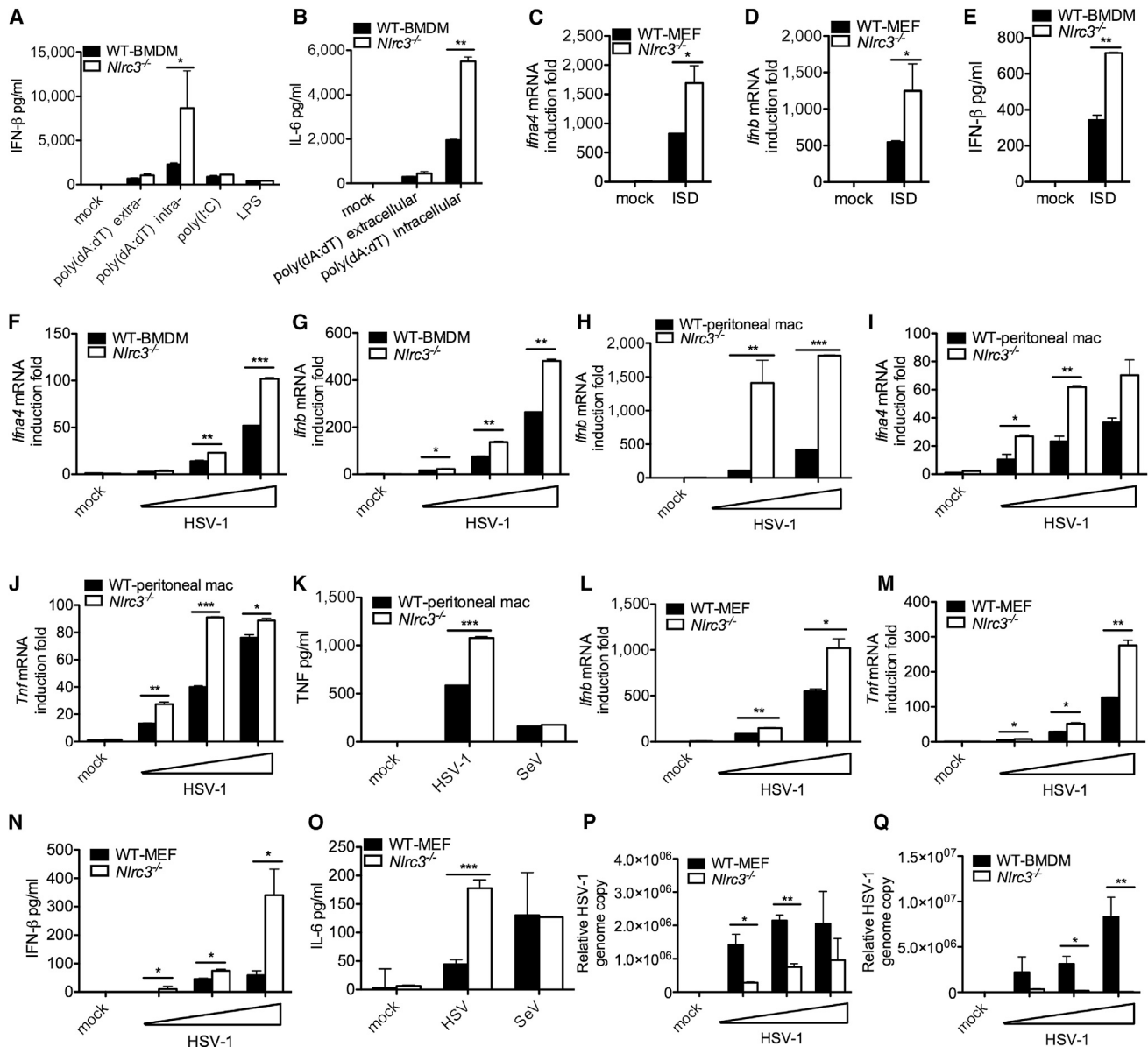


Figure 1. NLRC3 Attenuates DNA- and HSV-1-Induced Cytokines

(A and B) WT and *Nlrc3*^{-/-} BMDMs were transfected (intracellular) or incubated (extracellular) with poly(dA:dT), transfected with poly(I:C), or treated with LPS. IFN- β and IL-6 were measured 16 hr after treatment.

(C–E) *Nlrc3*^{+/+} and *Nlrc3*^{-/-} MEFs were transfected with ISD, and *Ifna4* (C) and *Ifnb* (D) transcripts or IFN- β (E) measured 6 hr after transfection.

HSV-1 was used at MOI 0.05, 0.1, and 1 for (F)–(J) unless specified.

(F and G) BMDMs were infected with HSV-1, and *Ifna4* (F) and *Ifnb1* (G) transcripts were measured.

(H–J) Peritoneal macrophages were infected with HSV-1, and *Ifna4* (H), *Ifnb1* (I), and *Tnf* (J) transcripts were measured.

(K) Peritoneal macrophages were infected with HSV-1 (MOI 1) or SeV (80 HA unit/ml) and TNF assayed.

(L and M) Primary MEFs were infected with HSV-1, and *Ifnb1* (L) and *Tnf* (M) transcripts were measured.

(N and O) Primary MEFs were infected with HSV-1, and IFN- β (N) and IL-6 (O) proteins were measured.

(P and Q) Primary MEFs (P) or BMDMs (Q) were infected with HSV-1, genomic DNA was extracted, and HSV relative genome copy number was determined by real-time PCR. All cytokines were determined by ELISA and transcripts determined by real-time PCR.

p* < 0.05, *p* < 0.01, ****p* < 0.001 (Student's *t* test). All data are representative of at least three independent experiments. See also Figures S1–S3.

NLRC3 Associates with STING and TBK1 and Alters the STING-TBK1 Interaction after Stimulation

To explore the mechanism by which NLRC3 interferes with STING and TBK1 function, we tested whether NLRC3 interacts

with STING and/or TBK1. Transient transfection and coimmunoprecipitation followed by immunoblot showed that HA-NLRC3 strongly associated with Flag-STING and more modestly with Flag-TBK1, but not with Flag-IRF3 (Figure 4A), suggesting that

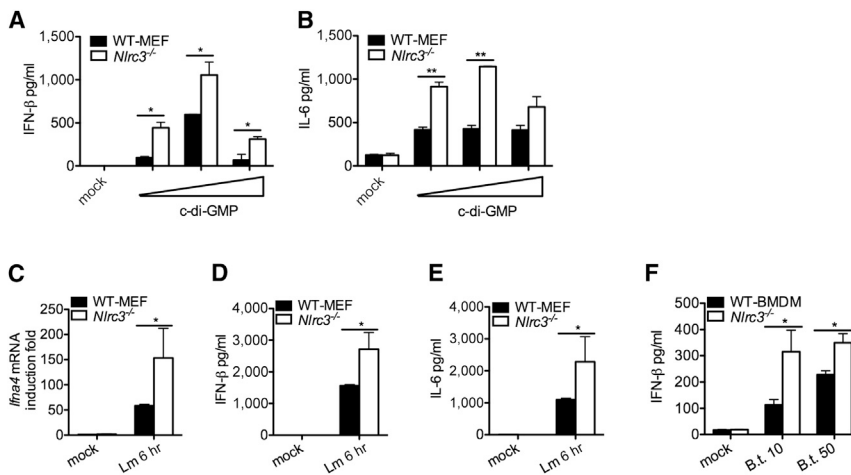


Figure 2. NLRC3 Deficiency Causes Increased IFN-β and IL-6 Production in Response to c-di-GMP

(A and B) c-di-GMP was transfected into primary MEFs, and IFN-β (A) and IL-6 (B) were measured 24 and 48 hr after transfection, respectively, by ELISA.

(C–E) Primary MEFs were infected with *L. monocytogenes* at MOI of 10, and *Irf4* transcripts (C) or IFN-β (D) and IL-6 (E) proteins were measured 6 hr after infection.

(F) BMDMs were infected with a second bacterial strain, *B. thailandensis*, and IFN-β was measured 6 hr after infection.

p* < 0.05, *p* < 0.01 (Student's *t* test). All data are representative of at least three independent experiments.

it interacts with the upstream STING-TBK1 complex but not with the downstream IRF3. This agrees with earlier data indicating that NLRC3 affected STING and TBK1 function but not IRF3 function (Figure 3A). Immunoblot of the input protein indicates that all of the proteins are expressed in readily detectable amounts (Figure 4A, right). In a more physiologic approach, HA-NLRC3 also associated with endogenous STING (Figure 4B, top) and TBK1 (Figure 4C) in a hemiendogenous system, but not with IRF3 (data not shown). These experiments indicate that NLRC3 can associate with STING and TBK1.

To further investigate whether the association between NLRC3 and STING is direct, we prepared purified, recombinant full-length NLRC3 and truncated STING protein (amino acid 139–379 and 139–344) and performed a protein pull-down assay. The results show that NLRC3 and STING directly bind to each other in a reciprocal pull-down assay (Figures 4D and 4E).

Next, a domain-mapping experiment was conducted with NLRC3 deletion constructs (Figure 4F). Full-length NLRC3, CARD-NBD, and NBD alone strongly associated with STING, whereas the CARD or LRR domain alone either did not associate, or did not associate strongly, with STING (Figure 4F). The CARD domain alone did not express in high amounts, but a prolonged exposure did not reveal any interaction (not shown). The presence of LRR reduced the association of NBD with STING, suggesting that the LRR is an inhibitory domain. These data indicate that the primary interaction domain in NLRC3 is the region that includes the NBD domain. A reciprocal experiment was performed to map the interaction domain in STING (Figure 4G). The first 240 residues of the N terminus or the C-terminal 111–379 residues did not interact with NLRC3, whereas the C-terminal residues 81–379 interacted with NLRC3. This indicates that the STING C-terminal soluble tail and residues 81–111 are required for interaction with NLRC3. The C-terminal residues 139–344 were shown to directly bind NLRC3 as demonstrated in Figures 4D and 4E; therefore, this region contains residues necessary and sufficient for association with NLRC3. However, a confounding issue with STING is that it is membrane bound and the transmembrane domain is required for STING localization to the ER. To examine this with the truncation mutants, we performed subcellular fractionation assay and showed that truncations 41–379 and 81–379 are membrane associated

whereas 111–379 and 221–379 lose their membrane localization, indicating that residues 81–111 contained a sequence important for membrane localization (Figure S4A). These results indicate that only the membrane-associated form of STING interacted with NLRC3. The interaction of STING with TBK1 produced the same results: STING truncation mutant 81–379 but not 111–379 interacted with TBK1 (Figure S4B), which is also consistent with previous findings (Zhong et al., 2008). We also mapped the domains on TBK1 that bind to NLRC3. The result shows that the N terminus of TBK-1, which contained the kinase domain, is required for NLRC3 association (Figure 4H).

Upon DNA stimulation, the association of STING with TBK1 is essential to activate downstream signals (Ishikawa and Barber, 2008; Sun et al., 2009; Tanaka and Chen, 2012; Zhong et al., 2008). Therefore, we tested whether the presence of NLRC3 interfered with the association of STING and TBK1. To pursue this in a physiologic system that did not involve overexpressed proteins, the association of STING and TBK1 was tested in *Nlrc3*^{-/-} and control BMDMs in response to HSV-1 infection. The avoidance of overexpressed protein for this analysis is because overexpressed NLRs are prone to artifacts. The results show stronger STING-TBK1 association in *Nlrc3*^{-/-} cells than in WT controls 2–4 hr after infection (Figure 4I, top; quantitation to the right). However, the association of STING-TBK1 was not enhanced by HSV-1. Because HSV-1 encodes a complex array of immune evasion and regulatory proteins that might obscure the outcome, we resort to ISD as a simplified system to examine responses to DNA without the confounding regulatory functions associated with HSV-1. The result shows enhanced STING-TBK1 association in WT cells after ISD stimulation, which was further potentiated in *Nlrc3*^{-/-} cells 2–4 hr after stimulation (Figure 4J, top; quantitation to the right). However, at the 6 hr time point, STING-TBK1 interaction was more pronounced in WT cells. These results indicate that NLRC3 interferes with STING-TBK1 association at the 2–4 hr time point.

NLRC3 Blocks STING Trafficking

STING has been shown to traffic from the ER to a perinuclear/golgi location and to endoplasmic-associated puncta after DNA stimulation (Ishikawa et al., 2009; Saitoh et al., 2009).

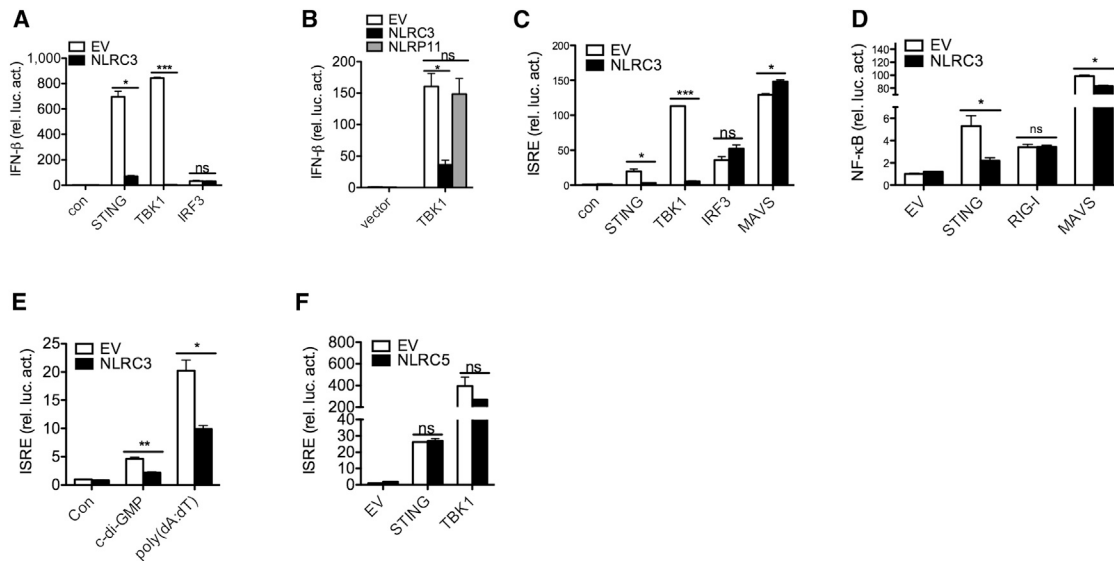


Figure 3. NLRC3 Suppresses STING-TBK1-Mediated IFN- β , ISRE, and NF- κ B Reporter Activation

(A–D) HEK293T cells were transfected with the IFN- β (A, B), ISRE (C), or NF- κ B (D) promoter reporter with the internal control Renilla luciferase reporter pLR-TK and empty vector or NLRC3 plasmid as indicated. Luciferase assays were performed 24 hr after transfection.

(E) HEK293T cells were transfected with the ISRE promoter reporter with the internal control Renilla luciferase reporter pLR-TK. Stimulatory ligands were transfected 24 hr after plasmid transfection. Luciferase assays were performed 16 hr after ligand stimulation.

(F) Same as (A)–(D), except cells were transfected with empty vector or NLRC5.

* $p < 0.05$, ** $p < 0.01$, *** $p < 0.001$ (Student's t test). Data are representative of at least two independent experiments.

STING is reported to colocalize with TBK1 at these puncta, which represent the proposed platform for TBK1-mediated IRF3 activation. In cells transfected with an empty vector (EV), ISD caused STING to present in a perinuclear pattern (Figure 5Aii) followed by a punctated appearance (Figure 5Aiii). However, the presence of NLRC3 dramatically reduced the trafficking of STING to the perinuclear region (12-fold) (Figure 5Av) and completely prevented STING's movement to puncta (Figure 5Avi). Thus, NLRC3 reduces STING trafficking after ISD stimulation.

To further pursue this finding by a biochemical approach, we examined whether the absence of NLRC3 affected STING and TBK1 colocalization by fast protein liquid chromatography (FPLC). This was performed with cell lysates prepared from HSV-1-infected and uninfected WT and *Nlrc3*^{-/-} primary MEFs. Similar to Figures 4I and 4J, this strategy did not involve any overexpressed proteins, thereby providing a physiologically relevant condition to test the impact of NLRC3 on STING and TBK1. Whole-cell lysates were fractionated by FPLC followed by immunoblotting of the fractions for STING and TBK1. In mock, uninfected wild-type controls (Figure 5B, top four rows, densitometry results in Figure 5C, left, quantitation in Figure 5D), a majority of TBK1 and STING resided in different fractions and only a small portion of STING and TBK1 was detected in the same fractions. In uninfected *Nlrc3*^{-/-} cells, 2.09-fold more STING and TBK1 were found in the same fractions compared to wild-type controls. Upon HSV-1 stimulation, 4.41-fold more STING and TBK1 were detected in the same fractions in *Nlrc3*^{-/-} cells than controls (Figure 5B, bottom four rows, densitometry results in Figure 5C, right, quantitation in Figure 5D).

The cumulative data in this figure are consistent with a model where NLRC3 interacts with STING and TBK1 to impede the interaction, because removal of NLRC3 by gene deletion led to more association of these two proteins. The inhibitory effect of NLRC3 on STING-TBK1 association was observed at the uninfected state and became more pronounced upon HSV-1 infection.

Nlrc3^{-/-} Cells Exhibit Elevated Signal Transduction after HSV-1 Infection

To search for changes in downstream signals that are known to be activated by STING and TBK1, we looked for changes in protein phosphorylation that lie downstream of STING activation after HSV-1 infection. Phosphorylation of TBK1, IRF3, p65, and JNK were induced 4–6 hr after infection in wild-type controls (Figure 6A). The amount of phospho-TBK1 and phospho-IRF3 4–6 hr after infection were higher in *Nlrc3*^{-/-} than control MEFs, and the phosphorylation of JNK was enhanced throughout all of the time points measured in *Nlrc3*^{-/-} cells. HSV-1 infection did not increase phosphorylation of ERK or p38, and NLRC3 did not alter these signals. HSV-1-infection-induced p65 nuclear translocation was also visualized by confocal microscopy and was found to be significantly augmented in *Nlrc3*^{-/-} cells (Figure 6B). Our earlier data indicate that NLRC3 affected the sensing of intracellular DNA. To study whether downstream signals induced by DNA are affected by NLRC3, we assessed phosphorylation induced by ISD transfected into MEFs. Intracellular ISD caused increased phosphorylation of TBK1 and JNK, but not ERK, in wild-type controls, and these responses were further augmented

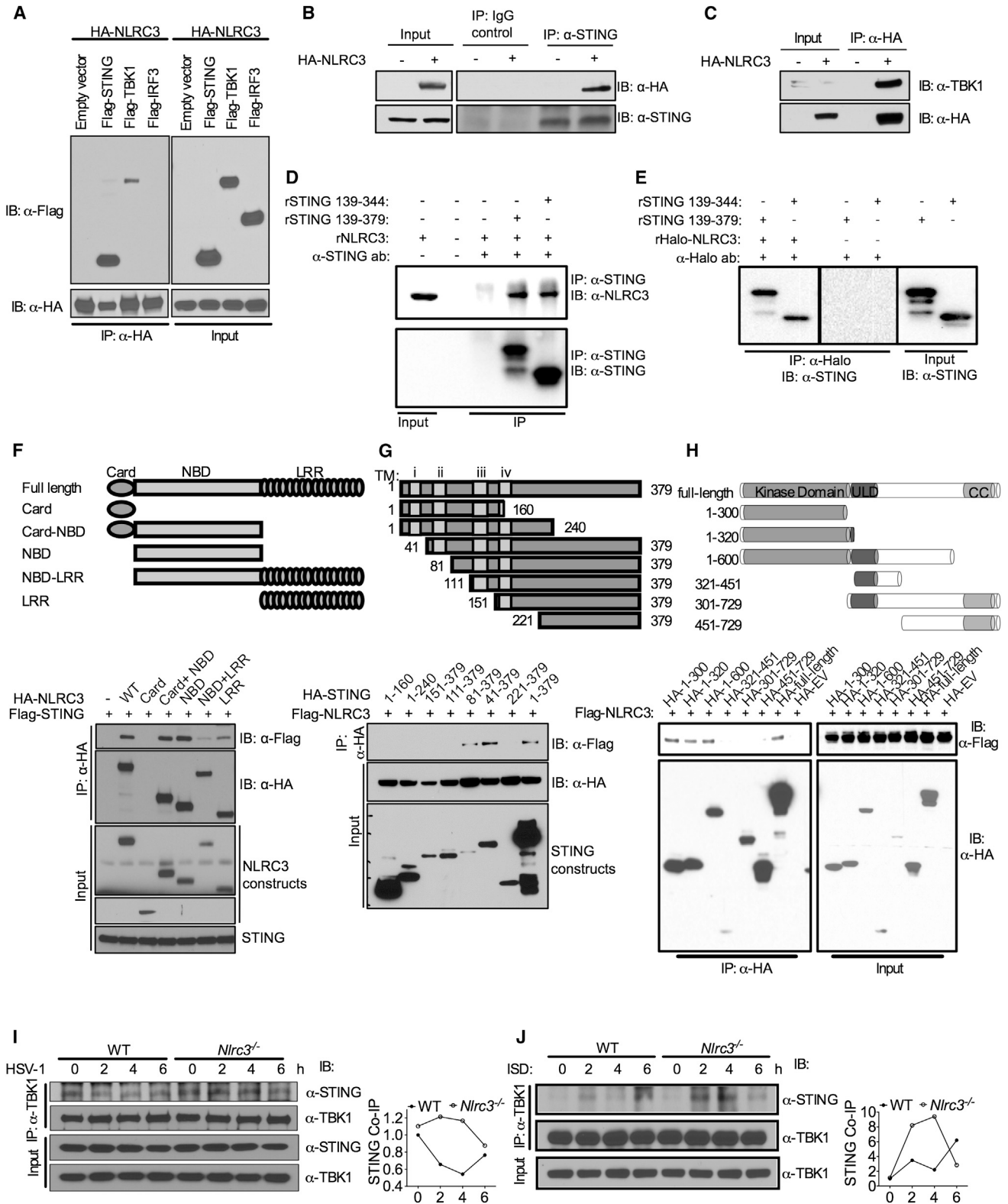


Figure 4. NLRC3 Associates with STING and TBK1 to Interfere with Their Interaction

(A) HEK293T cells were transfected with indicated plasmids and coimmunoprecipitation assay was performed 24 hr after transfection.

(B and C) HEK293T cells were transfected with HA-tagged NLRC3 (B) or empty vector (C).

Immunoprecipitation and immunoblots in (A)–(C) were performed with indicated antibodies.

(legend continued on next page)

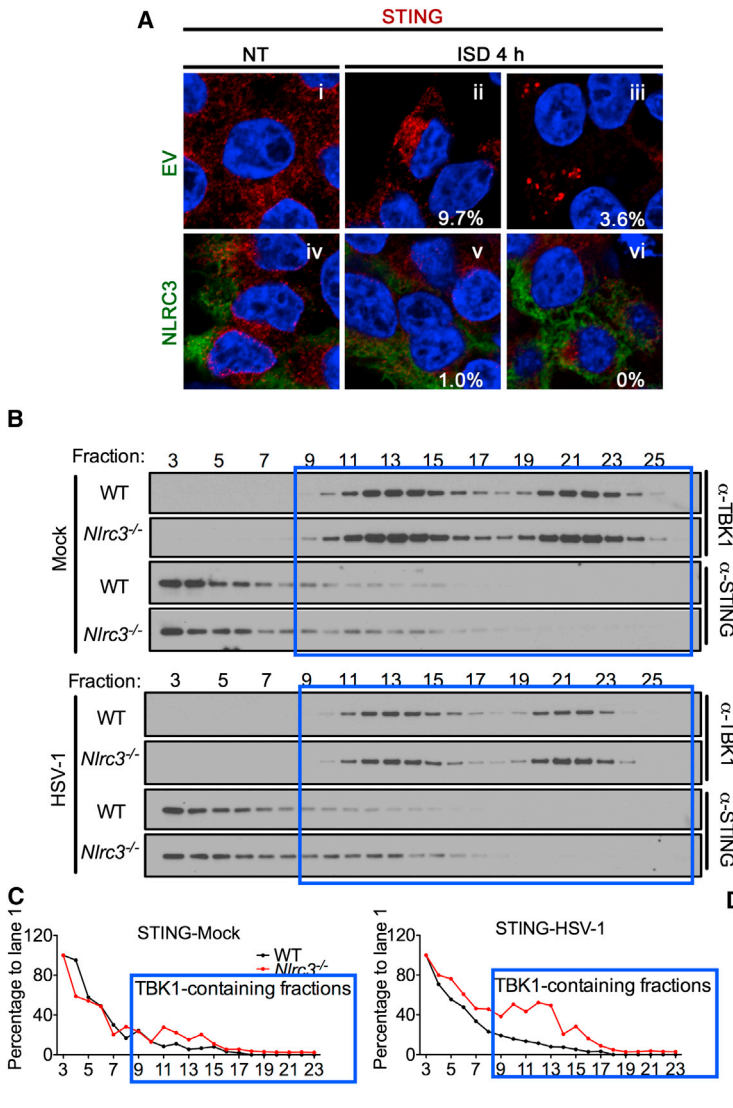


Figure 5. NLRC3 Blocks STING Trafficking

(A) HEK293T cells were transfected with STING with an empty vector (EV) or with NLRC3 followed by stimulation with ISD. The percentages indicate the number of cells showing STING localized to the perinuclear region (ii and v) or forming puncta (iii and vi). A minimum of 100 cells were counted per group.

(B) WT and *Nlrc3*^{-/-} MEFs were mock-treated or infected with HSV-1 (MOI = 1) for 4 hr. Cell lysate were subjected to FPLC, and fractions were collected and immunoblotted for STING and TBK1. The blue boxes indicate fractions that contained both TBK1 and STING.

(C) Densitometric tracing of STING in WT (black line) and *Nlrc3*^{-/-} cells (red) was performed with ImageJ.

(D) The areas depicted in (C) were calculated by area under curve in Prism. The areas where STING-TBK1 were localized in the same fractions are depicted for uninfected WT and *Nlrc3*^{-/-} MEFs and for HSV-1-infected WT and *Nlrc3*^{-/-} MEFs. In each case, the value for WT cells was set as 1.0. Data are representative of two independent experiments.

and S5B). TRAF6 also did not associate with STING in co-IP assays (Figure S5C).

NLRC3 Deficiency Augments Host Response to HSV-1 In Vivo

Next, to examine the in vivo importance of NLRC3, *Nlrc3*^{-/-} and control mice were infected intravenously (i.v.) with HSV-1 and survival, weight change, and morbidity were monitored (Figures 7A and 7B). Infected control mice exhibited significant lethargy and lack of movement (Movie S1), whereas infected *Nlrc3*^{-/-} mice were active and mobile (Movie S2). Many control mice had to be euthanized

in *Nlrc3*^{-/-} cells, supporting the model that NLRC3 regulates signaling responses caused by intracellular DNA (Figure 6C). As a specificity control, intracellular poly(I:C) was transfected into cells, and it did not cause increases in the phosphorylation of multiple key pathways in *Nlrc3*^{-/-} cells relative to controls (Figure 6D). These data suggest that NLRC3 is a negative regulator of innate immune signals generated upon HSV-1 infection and ISD stimulation. However, this function of NLRC3 is distinct from its regulation of NF- κ B signaling induced by TRAF6 during an LPS response (Schneider et al., 2012), because TRAF6 was not required for HSV-1-induced IFN-I activation (Figures S5A

6–8 days after infection when their body temperature was <32°C, whereas 100% of similarly infected *Nlrc3*^{-/-} mice showed a more modest temperature drop, ranging from 34.2°C to 35.9°C. Control mice also exhibited rapid weight loss after HSV-1 infection and had to be sacrificed because of a >20% weight loss. In contrast, *Nlrc3*^{-/-} mice maximally lost up to 11% of body weight and recovered 100% of body weight by day 9. Sera from HSV-1-infected *Nlrc3*^{-/-} mice showed increased IFN- β , TNF, and IL-6 6 hr after infection when compared to controls (Figures 7C–7E). HSV-1 genomic DNA copy number was significantly reduced in *Nlrc3*^{-/-} mice (Figure 7F). In

(D and E) Recombinant NLRC3 (D) and STING (E) in vitro binding assay was performed. Immunoblots were performed with the antibodies indicated. (F–H) HEK293T cells were transfected with indicated plasmids; constructs are shown at the top, the corresponding blots are shown below. The smaller peptides in (G) produced by 1–379 might be degradative products. (I and J) WT and *Nlrc3*^{-/-} BMDMs were infected with HSV-1 (I) or stimulated with ISD (J); immunoprecipitation and immunoblot were performed with the indicated antibodies at the indicated time points. Densitometric measurements of STING-TBK1 coprecipitation are shown to the right of each immunoblot. Data are representative of at least three independent experiments. See also Figures S4 and S5.

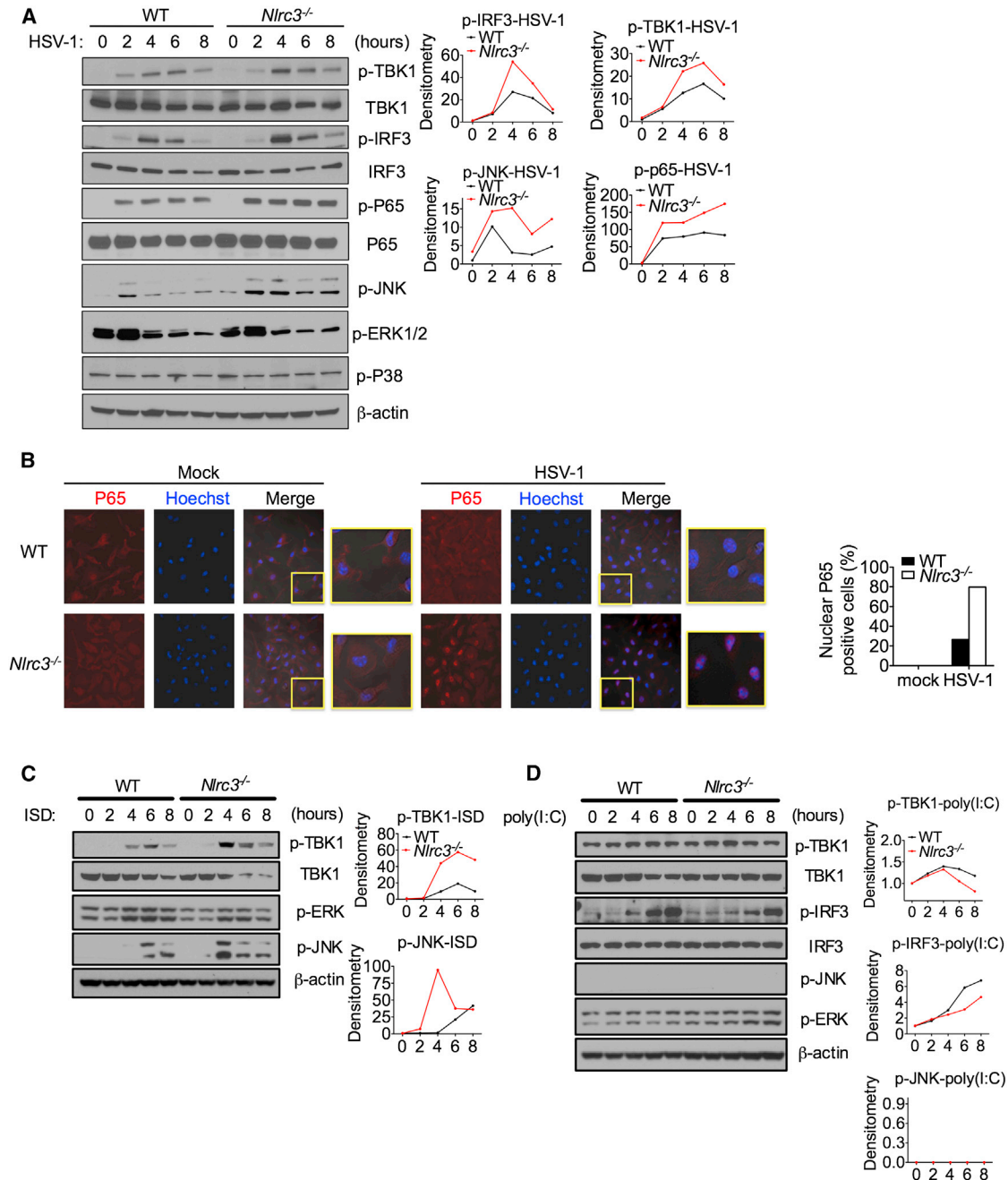


Figure 6. NLRC3 Deficiency Enhances Immune Signaling

(A) Immunoblot of phosphorylated (p-) TBK1, IRF3, p65, JNK, ERK, and p38 in lysates of WT and *Nlrc3*^{-/-} MEFs infected with HSV-1 (MOI 1) for indicated time points. Densitometric measurements are depicted to the right.

(B) BMDMs isolated from WT or *Nlrc3*^{-/-} mice were infected with HSV-1 (MOI 1) for 2.5 hr. Cells were fixed and stained for endogenous p65 (red) or Hoechst, which stains the nucleus (blue). The merged purple color is indicative of nuclear p65.

(C) Similar to (A), except cells were transfected with ISD.

(D) Similar to (A), except cells were transfected with poly(I:C).

Data are representative of at least two independent experiments.

contrast, weight loss or serum IFN-β level in *Nlrc3*^{-/-} mice was not significantly different from WT mice after infection with VSV (Figure S6). Thus, NLRC3 attenuates physiologic host response to HSV-1, a DNA virus, but not VSV, a RNA virus.

DISCUSSION

This study identifies NLRC3 as a negative regulator of type I IFN and proinflammatory cytokine production triggered by

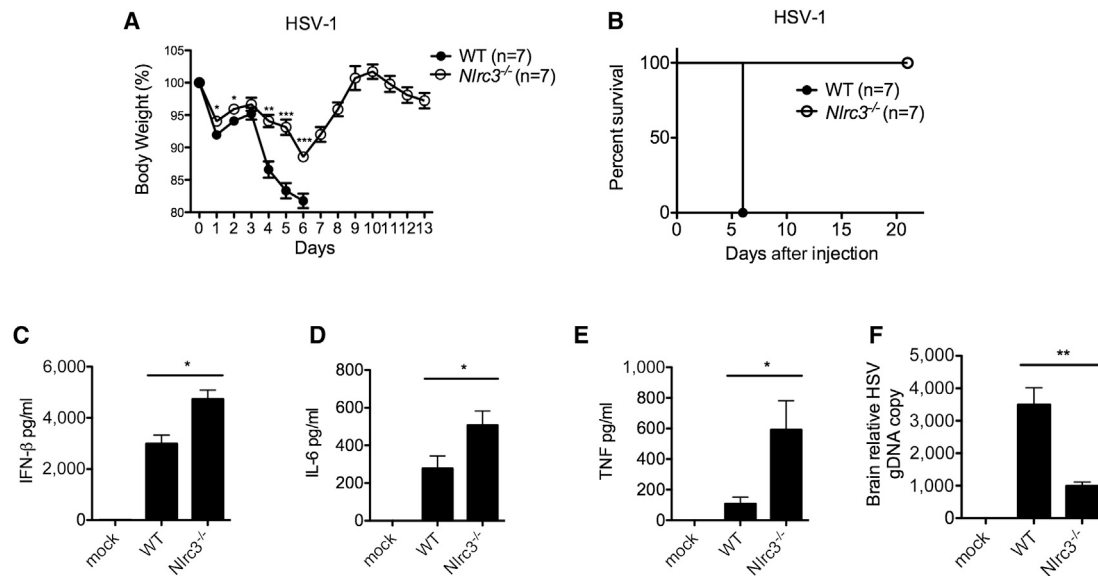


Figure 7. *Nlrc3*^{-/-} Mice Are More Resistant to HSV-1 Infection

WT and *Nlrc3*^{-/-} mice were infected i.v. with HSV-1 (2×10^7 pfu) and tested for (A) body weight, (B) survival rate, (C–E) serum cytokines (6 hr after infection), and (F) HSV-1 genomic DNA (harvested 5 days after infection and measured by real-time PCR analysis). * $p < 0.05$, ** $p < 0.01$, *** $p < 0.001$ (Student's t test). Data are representative of at least three independent experiments.

See also [Figure S6](#) and [Movies S1](#) and [S2](#).

cytoplasmic DNA and HSV-1. It also reduced the response caused by c-di-GMP, which provided us with the clue that linked NLRC3 to the STING pathway. Mechanistically, NLRC3 inhibits type I IFN promoter activation by STING and TBK, but not by the RIG-I-MAVS pathway. NLRC3 can directly interact with STING to reduce STING-TBK1 association, which is normally required for interferon induction. Furthermore, NLRC3 blocks ISD-induced STING trafficking to perinuclear and punctated regions, which is important for signal transduction downstream of STING (Ishikawa et al., 2009; Saitoh et al., 2009). Ablation of *Nlrc3* led to enhanced antiviral cytokine production and viral clearance in culture. Most important, HSV-1-infected *Nlrc3*^{-/-} mice exhibited greatly reduced morbidity, enhanced interferon and cytokine production, and reduced viral load. This work demonstrates that NLRC3 is a negative regulator of innate immunity triggered by the STING pathway.

There are multiple papers by several groups that identify the negative regulatory functions of NLRs. Studies of gene deletion strains show that NLRX1 inhibits RNA virus and LPS-induced cytokines in a cell-specific fashion (Allen et al., 2011; Xia et al., 2011), that NLRP12 reduces canonical and noncanonical NF- κ B (Allen et al., 2012; Zaki et al., 2011), that NLRP6 impedes MAPK and NF- κ B activation (Anand et al., 2012), and that NLRC5 inhibits NF- κ B and MAPK activation in some, but not all, gene deletion strains (Cui et al., 2010; Kumar et al., 2011). In addition, an in vitro study shows that NLRP4 reduces IFN-I production induced by nucleic acids (Cui et al., 2012). These findings indicate a broad function for NLRs in attenuating innate immune responses. However, none of the previously studied NLRs have been linked to the STING-mediated DNA-sensing pathway.

Whereas our previous work showed a function of NLRC3 in reducing the activation of TRAF6 in response to LPS (Schneider et al., 2012), this report shows that intracellular DNA sensing during HSV-1 infection is independent of TRAF6. Furthermore, the present report also shows that NLRC3 does not affect IFN-I induction by LPS. Thus, the impact of NLRC3 on LPS-induced cytokines such as TNF and IL-6 shown in our previous work (Schneider et al., 2012) probably occurs via a different path from IFN-I production caused by intracellular DNA. However, a recent paper indicates that TRAF6 is involved in cellular response to DNA and RNA (Konno et al., 2009). This might explain the more robust impact of NLRC3 in some experiments that used ISD instead of HSV-1. Further investigation is needed to fully assess the contribution of each pathway in response to nucleic acids in a NLRC3-dependent fashion.

The involvement of NLRC3 in two different responses (LPS-induced proinflammatory cytokines and intracellular DNA-induced IFN-I response) is in line with other NLRs, which serve multiple functions. For example, NLRP3 and NLRP1 are involved in inflammasome function and also in pyroptosis (Eisenbarth and Flavell, 2009; Kovarova et al., 2012; Masters et al., 2012). NOD2 activates NF- κ B, MAVS-induced type I IFN, and autophagy (Cooney et al., 2010; Homer et al., 2010; Sabbah et al., 2009; Travassos et al., 2010). NLRP6 mediates inflammasome activation (Elinav et al., 2011), inhibits NF- κ B activation (Anand et al., 2012), and promotes epithelium repair and renewal (Chen et al., 2011; Normand et al., 2011).

It is well accepted that cytosolic DNA is immune stimulatory and that STING is the central adaptor protein for multiple intracellular DNA-sensing pathways (Ishikawa and Barber, 2008; Ishikawa et al., 2009; Jin et al., 2008; Sun et al., 2009; Zhong et al., 2008). Additionally, STING also mediates responses to

RNA (Ishikawa et al., 2009; Sun et al., 2009; Zhong et al., 2008), cyclic dinucleotides (Jin et al., 2011; Sauer et al., 2011), cyclic GMP-AMP (Wu et al., 2013), and bacterial (Gratz et al., 2011; Ishikawa and Barber, 2008; Ishikawa et al., 2009; Jin et al., 2011; Manzanillo et al., 2012; Watson et al., 2012), viral (Holm et al., 2012; Ishikawa and Barber, 2008; Ishikawa et al., 2009; Sun et al., 2009; Zhong et al., 2008), eukaryotic pathogen-derived (Sharma et al., 2011), and self (Gall et al., 2012) DNA. It also intersects with other DNA sensors such as IFI16 and DDX41 (Unterholzner et al., 2010; Zhang et al., 2011). Therefore, it is significant that NLRC3 impacts this central DNA-sensing molecule. In contrast to its intersection with STING-TBK1, we have not found a direct effect of NLRC3 on IFI16 or DDX41 (not shown). We also have not found a consistent function for NLRC3 in altering host response to intracellular poly(I:C) or the RNA viruses tested. Although previous work has shown a consistent role for STING in host response to DNA virus, the results are less consistent for RNA virus. For example, IFN- β production and IRF3 nuclear translocation status are comparable between VSV-infected WT and *Sting*^{-/-} MEFs and BMDMs, whereas *Sting*^{-/-} dendritic cells produced less IFN- α after VSV infection (Ishikawa et al., 2009). It is possible that an investigation of IFN- α in dendritic cells might reveal a function for NLRC3 in response to VSV. It is also possible that NLRC3 inhibits RNA virus in a time- and dose-dependent fashion that was missed. Finally, NLRC3 only partially shuts off STING function, and therefore residual function might promote anti-RNA viral response.

The main finding of this work is that NLRC3 interacts with STING biochemically and functionally. It would follow that NLRC3 should reduce signals that lie downstream of STING activation. This is supported by the observation that *Nlrc3*^{-/-} cells showed increased p-IRF3 (Figure 6A) and NF- κ B phosphorylation/translocation (Figures 6A and 6B) after HSV-1 infection. The luciferase data showed that NLRC3 did not affect IRF3 activation of an ISRE promoter; hence, the impact of NLRC3 is not directly on IRF3. We further showed that NLRC3 affected NF- κ B activation by STING but not RIG-I or MAVS (Figure 3D), and therefore NLRC3 did not indiscriminately inhibit NF- κ B activation. Instead, it inhibited NF- κ B activation only downstream of STING activation. Together, these data lead to the conclusion that NLRC3 negatively impacts STING, which then affects downstream events such as IRF3 and NF- κ B activation.

In addition to pathogen-driven responses, DNA-dependent immune response triggered by self-DNA is associated with several diseases. As an example, DNase II-deficient mice were unable to digest self-DNA from apoptotic cells, and mice lacking DNase II died during embryonic development partly because of anemia (Kawane et al., 2001), which was rescued when STING was also removed (Ahn et al., 2012). This suggests that the cytosolic DNA-sensing pathway is involved in the pathology evoked by DNA sensing by STING.

In summary, our findings show the attenuation of DNA and c-di-GMP sensing by NLRC3 and reveal the intersection two pivotal pathways, NLR and STING, in the control of innate immune responses. This work expands the function of NLRs to the important task of regulating host response elicited by intracellular DNA and c-di-GMP.

EXPERIMENTAL PROCEDURES

Cell Culture

HEK293T cells were purchased from ATCC and maintained in DMEM (GIBCO) supplemented with 10% fetal bovine serum, 1% penicillin, and 100 μ g/ml streptomycin. *Nlrc3*^{+/+} and *Nlrc3*^{-/-} MEFs were generated from 13.5-day embryos and maintained in the complete DMEM medium described above with 1 mM sodium pyruvate, 4 mM L-glutamine, and nonessential amino acid. BMDMs were generated in the presence of L-929 conditional medium as previously described. All cells were grown in a 37°C incubator supplied with 5% CO₂.

Reagents and Antibodies

poly(dA:dT) was purchased from InvivoGen, c-di-GMP from KeraFast, cytotoxicity detection kit from Roche, HSV-1 (KOS strain) from ATCC and propagated in Vero cells, Sendai virus (Cantell strain) from Charles River, and VSV (Indiana strain) from ATCC and propagated in Vero cells. TNF and IL-6 ELISA kits were from BD Biosciences, mouse anti-IFN- β antibody was from Cosmo Bio, anti-IFN- β was from R&D Systems, anti-phospho-TBK1, TBK1, phospho-IRF3, IRF3, phospho-p65, p65, phospho-JNK, phospho-ERK, and phospho-p38 were from Cell Signaling Technology, and anti- β -actin antibody was from Santa Cruz.

Experimental Animals and In Vivo Virus Infection

The C57BL/6 *Nlrc3*^{-/-} mice have been described (Schneider et al., 2012). C57BL/6 littermates were produced and used in selected experiments. Mice were treated in accordance with the National Institutes of Health *Guide for the Care and Use of Laboratory Animals* and the Institutional Animal Care and Use Committee of the University of North Carolina at Chapel Hill. Mice (8–10 weeks old) were infected with HSV-1 (2×10^7 pfu of viruses per mouse) or VSV (5×10^7 pfu of viruses per mouse) by intravenous injection. The temperature and weight of the mice were monitored accordingly. For cytokine studies, mice were sacrificed 6 hr after infection and sera were collected through cardiac puncture. For HSV-1 genome copy number measurement, brains were harvested 5 days after infection. For all experiments, wild-type and *Nlrc3*^{-/-} mice were matched for age and sex.

Plasmids and Molecular Cloning

FLAG-tagged STING (originally cloned and named as MITA) full-length and domain truncation expression plasmids have been described (Zhong et al., 2008). HA-tagged NLRC3 full-length and domain truncation expression plasmids were cloned into pcDNA3.1.

Real-Time RT-PCR

Total RNA was extracted and assayed by real-time PCR as described with SYBR green master mix or Tagman assay (Schneider et al., 2012). Primers used were as follows: mIFN β : 5'- ATGAGTGGTGGTTGCAGGC-3', 5'- ATGAGTGGTGGTTGCAGGC-3'; mIFN- α 4: 5'- CCTGTGTGATGCAGGAACC-3', 5'- TCACCTCCCAGGCACAGA-3'; actin: 5'- AGGCTATGCTCTCCCTCAC-3', 5'- CTCTCAGCTGTGGTGGTAA-3'; mTNF: Mm00443258_m1, mL-6: Mm00446190_m1.

HSV-1 Genomic DNA Copy-Number Measurement

Genomic DNA was extracted with DNeasy Blood & Tissue Kit (QIAGEN) according to manufacturer's protocol. HSV-1 genomic DNA copy numbers were then determined by real-time PCR with HSV-1-specific primer: 5'-TG GGACACATGCCTCTTGG-3', 5'-ACCCTTAGTCAGACTCTGTACTTACCC-3'.

Virus, Bacteria Infection, and poly(dA:dT) Stimulation

BMDMs or MEFs were plated in 24-well plates and grown to 80% confluence overnight. The cells were washed with PBS and infected with HSV-1 (KOS strain), SeV (Cantell strain), or VSV (Indiana strain) at the indicated multiplicity of infection (MOI) at 37°C in serum-free DMEM for 1 hr. The cells were then washed with warm PBS and cultured in complete DMEM.

L. monocytogenes (43251) or *B. thailandensis* were grown to log phase and added to the cell cultures at a MOI of 10. After 30 min, gentamicin (50 μ g/ml; Life Technologies) was added to the medium. The medium was changed after 1 hr of infection. poly(dA:dT), poly(I:C), or ISD were added or transfected with

lipofectamine 2000 (Invitrogen) at 4 $\mu\text{g}/\text{ml}$ to BMDMs or MEFs for the indicated time. LPS were added into cell culture at 100 ng/ml. c-di-GMP were transfected at 1 $\mu\text{g}/\text{ml}$, 2 $\mu\text{g}/\text{ml}$, or 4 $\mu\text{g}/\text{ml}$.

Coimmunoprecipitation

Procedures were done as previously described (Schneider et al., 2012).

Transfection and Luciferase Reporter Analysis

HEK293T cells were seeded in 24-well plates at the density of 1.0×10^5 per well and transfected the following day by lipofectamine 2000 according to the manufacturer's instruction. 10 ng of pRT-TK Renilla luciferase reporter plasmid and 100 ng of firefly luciferase reporter plasmids were transfected together with indicated expression plasmids. Luciferase activity was measured 24 hr after transfection via the Dual-Glo Luciferase Assay System.

Recombinant Protein Purification and In Vitro Pull-Down

Recombinant baculovirus expressing NLRC3 carrying an N-terminal Halo-Tag (HALO) and C-terminal hexahistidine tag (6XHIS) was generated as described by Mo et al. (2012). For assays with immobilized Halo ligand capture (HaloLink, Promega) for protein capture, recombinant HALO-NLRC3-6XHIS was partially purified by immobilized Ni^{2+} chromatography (PrepEase Ni-TED, USB). HaloLink resin or HaloLink resin incubated with 1 μg of HALO-NLRC3-6XHIS was added to IP buffer containing 50 mM HEPES (pH 7.5), 150 mM NaCl, 5 mM β -mercaptoethanol, and 0.1% CHAPS and 1 μg of recombinant STING protein (Ouyang et al., 2012). After 4 hr rotating at 4°C, the HALO-resin-associated proteins were isolated by centrifugation for 30 s at 13,000 \times g and the resins were washed three times with IP buffer supplemented with 300 mM NaCl. The resin-associated STING proteins were liberated with 1 \times SDS-PAGE loading buffer and analyzed by immunoblot analysis. For assays with anti-STING antibody, coimmunoprecipitation tag-free NLRC3 was purified to near homogeneity via tandem immobilized Ni^{2+} chromatography and HALO-ligand affinity chromatography followed by TEV-protease treatment to remove both the HALO and 6XHIS as previously described. Purified NLRC3 (1 μg) and purified STING proteins (1 μg) were combined in IP buffer and incubated with anti-STING antibody while rotating at 4°C overnight. The STING protein and associated NLRC3 were captured by protein A paramagnetic beads (Miltenyi) according to the manufacturer's protocols and assayed by immunoblot for STING (Cell Signaling) and NLRC3 (Sigma) as described.

Fast Protein Liquid Chromatography

Nlrc3^{+/+} or *Nlrc3*^{-/-} MEFs were harvested after indicated treatment and lysed in hypotonic buffer (25 mM Tris-HCl [pH 7.5], 2 mM DTT) with a dounce homogenizer on ice. The lysate was then centrifuged at 16,000 \times g for 10 min. The precipitate was lysed in CHAPS buffer (50 mM Tris-HCl [pH 7.5], 150 mM NaCl, 1 mM DTT, 0.5 mM EDTA, 5% glycerol, and 0.1% CHAPS) with a dounce homogenizer on ice and then centrifuged at 16,000 \times g for 10 min. The protein concentrations of the supernatant were determined by Bio-Rad Protein Assay. Equal amount of protein from *Nlrc3*^{+/+} or *Nlrc3*^{-/-} cells were subjected to size exclusion chromatography (Superose 6). The indicated fractions were subjected to immunoblot analysis with the indicated antibodies. Densitometry for immunoblot was performed with ImageJ.

Confocal Microscopy

Nlrc3^{+/+} or *Nlrc3*^{-/-} BMDMs (4×10^5) were seeded onto coverslips in 24-well dishes and were grown overnight before inoculation with HSV-1 at the MOI of 1 for 3 hr. Cells were fixed with 4% paraformaldehyde (PFA), followed by ice-cold methanol. Cells were stained with anti-p65 (D14E12; Cell Signaling) and Alexa Fluor 546-conjugated anti-rabbit antibody (A-11035; Invitrogen) and then were counterstained for nucleic acids with Hoechst 33342. In experiments with overexpressed protein, HEK293T cells (2.5×10^5) were reverse transfected with Lipofectamine 2000 with STING-HA (100 μg) and NLRC3-FLAG (375 μg) directly onto poly-L-lysine-coated coverslips. After 24 hr, cells were transfected with ISD (4 $\mu\text{g}/\text{ml}$) for 4 hr, followed by PFA fixation. Cells were stained with anti-HA (3724S; Cell Signaling) and anti-FLAG (F1804, Sigma) followed with AF546-conjugated anti-rabbit antibody and AF488-conjugated anti-mouse IgG1 antibody (A-11035 and A11029; Invitrogen) and

then counterstained for nucleic acids with Hoechst 33342. Cells were analyzed with a Zeiss LSM 710 laser-scanning confocal microscope.

Statistical Analysis

Statistical analysis was carried out with Prism 5.0 for Macintosh. All data are shown as mean \pm SD. The mean values for biochemical data from each group were compared by Student's t test. Comparisons between multiple time points were analyzed by repeated-measurements analysis of variance with Bonferroni post-tests. In all tests, p values of less than 0.05 were considered statistically significant. *p < 0.05, **p < 0.01, ***p < 0.001.

SUPPLEMENTAL INFORMATION

Supplemental Information includes six figures and two movies and can be found with this article online at <http://dx.doi.org/10.1016/j.immuni.2014.01.010>.

ACKNOWLEDGMENTS

Supported by NIH grants CA156330, P01DK094779, and R37-AI029564, (J.P.-Y.T.); AI088255 (J.A.D.); AI107810 (B.D.); and DE 018281 and U19 AI1099665 (B.D. and J.P.-Y.T.); Burroughs Wellcome Fund Career Award for Medical Scientists (J.A.D.); and MOST grants 2014CB910400 and 2013CB911103 and NSFC grants 31200559 and 31330019 (S.O. and Z.-J.L.). We thank T.W. Mak for sharing *Traf6*^{+/+}, *Traf6*^{+/-}, and *Traf6*^{-/-} cells, A. Baldwin and L. Su for materials, E. Miao for *Burkholderia thailandensis*, and R. Chen for support and discussion.

Received: August 29, 2013

Accepted: January 7, 2014

Published: February 20, 2014

REFERENCES

- Ahn, J., Gutman, D., Saijo, S., and Barber, G.N. (2012). STING manifests self DNA-dependent inflammatory disease. *Proc. Natl. Acad. Sci. USA* 109, 19386–19391.
- Allen, I.C., Moore, C.B., Schneider, M., Lei, Y., Davis, B.K., Scull, M.A., Gris, D., Roney, K.E., Zimmermann, A.G., Bowzard, J.B., et al. (2011). NLRX1 protein attenuates inflammatory responses to infection by interfering with the RIG-I-MAVS and TRAF6-NF- κ B signaling pathways. *Immunity* 34, 854–865.
- Allen, I.C., Wilson, J.E., Schneider, M., Lich, J.D., Roberts, R.A., Arthur, J.C., Woodford, R.M., Davis, B.K., Uronis, J.M., Herfarth, H.H., et al. (2012). NLRP12 suppresses colon inflammation and tumorigenesis through the negative regulation of noncanonical NF- κ B signaling. *Immunity* 36, 742–754.
- Anand, P.K., Malireddi, R.K.S., Lukens, J.R., Vogel, P., Bertin, J., Lamkanfi, M., and Kanneganti, T.-D. (2012). NLRP6 negatively regulates innate immunity and host defence against bacterial pathogens. *Nature* 488, 389–393.
- Burdette, D.L., Monroe, K.M., Sotelo-Troha, K., Iwig, J.S., Eckert, B., Hyodo, M., Hayakawa, Y., and Vance, R.E. (2011). STING is a direct innate immune sensor of cyclic di-GMP. *Nature* 478, 515–518.
- Chen, G.Y., Liu, M., Wang, F., Bertin, J., and Núñez, G. (2011). A functional role for Nlrp6 in intestinal inflammation and tumorigenesis. *J. Immunol.* 186, 7187–7194.
- Chiu, Y.H., Macmillan, J.B., and Chen, Z.J. (2009). RNA polymerase III detects cytosolic DNA and induces type I interferons through the RIG-I pathway. *Cell* 138, 576–591.
- Cooney, R., Baker, J., Brain, O., Danis, B., Pichulik, T., Allan, P., Ferguson, D.J., Campbell, B.J., Jewell, D., and Simmons, A. (2010). NOD2 stimulation induces autophagy in dendritic cells influencing bacterial handling and antigen presentation. *Nat. Med.* 16, 90–97.
- Cui, J., Zhu, L., Xia, X., Wang, H.Y., Legras, X., Hong, J., Ji, J., Shen, P., Zheng, S., Chen, Z.J., and Wang, R.F. (2010). NLRC5 negatively regulates the NF- κ B and type I interferon signaling pathways. *Cell* 141, 483–496.

- Cui, J., Li, Y., Zhu, L., Liu, D., Songyang, Z., Wang, H.Y., and Wang, R.-F. (2012). NLPR4 negatively regulates type I interferon signaling by targeting the kinase TBK1 for degradation via the ubiquitin ligase DTX4. *Nat. Immunol.* **13**, 387–395.
- Eisenbarth, S.C., and Flavell, R.A. (2009). Innate instruction of adaptive immunity revisited: the inflammasome. *EMBO Mol. Med.* **1**, 92–98.
- Elinav, E., Strowig, T., Kau, A.L., Henao-Mejia, J., Thaiss, C.A., Booth, C.J., Peaper, D.R., Bertin, J., Eisenbarth, S.C., Gordon, J.I., and Flavell, R.A. (2011). NLPR6 inflammasome regulates colonic microbial ecology and risk for colitis. *Cell* **145**, 745–757.
- Gall, A., Treuting, P., Elkon, K.B., Loo, Y.M., Gale, M., Jr., Barber, G.N., and Stetson, D.B. (2012). Autoimmunity initiates in nonhematopoietic cells and progresses via lymphocytes in an interferon-dependent autoimmune disease. *Immunity* **36**, 120–131.
- Gratz, N., Hartweg, H., Matt, U., Kratochvill, F., Janos, M., Sigel, S., Drobits, B., Li, X.D., Knapp, S., and Kovarik, P. (2011). Type I interferon production induced by *Streptococcus pyogenes*-derived nucleic acids is required for host protection. *PLoS Pathog.* **7**, e1001345.
- Holm, C.K., Jensen, S.B., Jakobsen, M.R., Cheshenko, N., Horan, K.A., Moeller, H.B., Gonzalez-Dosal, R., Rasmussen, S.B., Christensen, M.H., Yarovinsky, T.O., et al. (2012). Virus-cell fusion as a trigger of innate immunity dependent on the adaptor STING. *Nat. Immunol.* **13**, 737–743.
- Homer, C.R., Richmond, A.L., Rebert, N.A., Achkar, J.P., and McDonald, C. (2010). ATG16L1 and NOD2 interact in an autophagy-dependent antibacterial pathway implicated in Crohn's disease pathogenesis. *Gastroenterology* **139**, 1630–1641.e1–e2.
- Huang, Y.-H., Liu, X.-Y., Du, X.-X., Jiang, Z.-F., and Su, X.-D. (2012). The structural basis for the sensing and binding of cyclic di-GMP by STING. *Nat. Struct. Mol. Biol.* **19**, 728–730.
- Ishikawa, H., and Barber, G.N. (2008). STING is an endoplasmic reticulum adaptor that facilitates innate immune signalling. *Nature* **455**, 674–678.
- Ishikawa, H., Ma, Z., and Barber, G.N. (2009). STING regulates intracellular DNA-mediated, type I interferon-dependent innate immunity. *Nature* **461**, 788–792.
- Jin, L., Waterman, P.M., Jonscher, K.R., Short, C.M., Reisdorph, N.A., and Cambier, J.C. (2008). MPYS, a novel membrane tetraspanner, is associated with major histocompatibility complex class II and mediates transduction of apoptotic signals. *Mol. Cell. Biol.* **28**, 5014–5026.
- Jin, L., Hill, K.K., Filak, H., Mogan, J., Knowles, H., Zhang, B., Perraud, A.-L., Cambier, J.C., and Lenz, L.L. (2011). MPYS is required for IFN response factor 3 activation and type I IFN production in the response of cultured phagocytes to bacterial second messengers cyclic-di-AMP and cyclic-di-GMP. *J. Immunol.* **187**, 2595–2601.
- Kawane, K., Fukuyama, H., Kondoh, G., Takeda, J., Ohsawa, Y., Uchiyama, Y., and Nagata, S. (2001). Requirement of DNase II for definitive erythropoiesis in the mouse fetal liver. *Science* **292**, 1546–1549.
- Konno, H., Yamamoto, T., Yamazaki, K., Gohda, J., Akiyama, T., Semba, K., Goto, H., Kato, A., Yujiri, T., Imai, T., et al. (2009). TRAF6 establishes innate immune responses by activating NF- κ B and IRF7 upon sensing cytosolic viral RNA and DNA. *PLoS ONE* **4**, e5674.
- Kovarova, M., Hesker, P.R., Jania, L., Nguyen, M., Snouwaert, J.N., Xiang, Z., Lommatzsch, S.E., Huang, M.T., Ting, J.P., and Koller, B.H. (2012). NLPR1-dependent pyroptosis leads to acute lung injury and morbidity in mice. *J. Immunol.* **189**, 2006–2016.
- Kumar, H., Pandey, S., Zou, J., Kumagai, Y., Takahashi, K., Akira, S., and Kawai, T. (2011). NLRC5 deficiency does not influence cytokine induction by virus and bacteria infections. *J. Immunol.* **186**, 994–1000.
- Manzanillo, P.S., Shiloh, M.U., Portnoy, D.A., and Cox, J.S. (2012). *Mycobacterium tuberculosis* activates the DNA-dependent cytosolic surveillance pathway within macrophages. *Cell Host Microbe* **11**, 469–480.
- Masters, S.L., Gerlic, M., Metcalf, D., Preston, S., Pellegrini, M., O'Donnell, J.A., McArthur, K., Baldwin, T.M., Chevrier, S., Nowell, C.J., et al. (2012). NLPR1 inflammasome activation induces pyroptosis of hematopoietic progenitor cells. *Immunity* **37**, 1009–1023.
- Mo, J., Boyle, J.P., Howard, C.B., Monie, T.P., Davis, B.K., and Duncan, J.A. (2012). Pathogen sensing by nucleotide-binding oligomerization domain-containing protein 2 (NOD2) is mediated by direct binding to muramyl dipeptide and ATP. *J. Biol. Chem.* **287**, 23057–23067.
- Normand, S., Delanoye-Crespin, A., Bressenot, A., Huot, L., Grandjean, T., Peyrin-Biroulet, L., Lemoine, Y., Hot, D., and Chamailard, M. (2011). Nod-like receptor pyrin domain-containing protein 6 (NLPR6) controls epithelial self-renewal and colorectal carcinogenesis upon injury. *Proc. Natl. Acad. Sci. USA* **108**, 9601–9606.
- Ouyang, S., Song, X., Wang, Y., Ru, H., Shaw, N., Jiang, Y., Niu, F., Zhu, Y., Qiu, W., Parvatiyar, K., et al. (2012). Structural analysis of the STING adaptor protein reveals a hydrophobic dimer interface and mode of cyclic di-GMP binding. *Immunity* **36**, 1073–1086.
- Sabbah, A., Chang, T.H., Harnack, R., Frohlich, V., Tominaga, K., Dube, P.H., Xiang, Y., and Bose, S. (2009). Activation of innate immune antiviral responses by Nod2. *Nat. Immunol.* **10**, 1073–1080.
- Saitoh, T., Fujita, N., Hayashi, T., Takahara, K., Satoh, T., Lee, H., Matsunaga, K., Kageyama, S., Omori, H., Noda, T., et al. (2009). Atg9a controls dsDNA-driven dynamic translocation of STING and the innate immune response. *Proc. Natl. Acad. Sci. USA* **106**, 20842–20846.
- Sauer, J.D., Sotelo-Troha, K., von Moltke, J., Monroe, K.M., Rae, C.S., Brubaker, S.W., Hyodo, M., Hayakawa, Y., Woodward, J.J., Portnoy, D.A., and Vance, R.E. (2011). The N-ethyl-N-nitrosourea-induced Goldenticket mouse mutant reveals an essential function of Sting in the in vivo interferon response to *Listeria monocytogenes* and cyclic dinucleotides. *Infect. Immun.* **79**, 688–694.
- Schneider, M., Zimmermann, A.G., Roberts, R.A., Zhang, L., Swanson, K.V., Wen, H., Davis, B.K., Allen, I.C., Holl, E.K., Ye, Z., et al. (2012). The innate immune sensor NLRC3 attenuates Toll-like receptor signaling via modification of the signaling adaptor TRAF6 and transcription factor NF- κ B. *Nat. Immunol.* **13**, 823–831.
- Shang, G., Zhu, D., Li, N., Zhang, J., Zhu, C., Lu, D., Liu, C., Yu, Q., Zhao, Y., Xu, S., and Gu, L. (2012). Crystal structures of STING protein reveal basis for recognition of cyclic di-GMP. *Nat. Struct. Mol. Biol.* **19**, 725–727.
- Sharma, S., DeOliveira, R.B., Kalantari, P., Parroche, P., Goutagny, N., Jiang, Z., Chan, J., Bartholomeu, D.C., Lauw, F., Hall, J.P., et al. (2011). Innate immune recognition of an AT-rich stem-loop DNA motif in the *Plasmodium falciparum* genome. *Immunity* **35**, 194–207.
- Shaw, P.J., Lamkanfi, M., and Kanneganti, T.D. (2010). NOD-like receptor (NLR) signaling beyond the inflammasome. *Eur. J. Immunol.* **40**, 624–627.
- Shu, C., Yi, G., Watts, T., Kao, C.C., and Li, P. (2012). Structure of STING bound to cyclic di-GMP reveals the mechanism of cyclic dinucleotide recognition by the immune system. *Nat. Struct. Mol. Biol.* **19**, 722–724.
- Stetson, D.B., and Medzhitov, R. (2006). Recognition of cytosolic DNA activates an IRF3-dependent innate immune response. *Immunity* **24**, 93–103.
- Sun, W., Li, Y., Chen, L., Chen, H., You, F., Zhou, X., Zhou, Y., Zhai, Z., Chen, D., and Jiang, Z. (2009). ERIS, an endoplasmic reticulum IFN stimulator, activates innate immune signaling through dimerization. *Proc. Natl. Acad. Sci. USA* **106**, 8653–8658.
- Takeuchi, O., and Akira, S. (2007). Recognition of viruses by innate immunity. *Immunol. Rev.* **220**, 214–224.
- Tanaka, Y., and Chen, Z.J. (2012). STING specifies IRF3 phosphorylation by TBK1 in the cytosolic DNA signaling pathway. *Sci. Signal.* **5**, ra20.
- Travassos, L.H., Carneiro, L.A., Ramjeet, M., Hussey, S., Kim, Y.G., Magalhães, J.G., Yuan, L., Soares, F., Chea, E., Le Bourhis, L., et al. (2010). Nod1 and Nod2 direct autophagy by recruiting ATG16L1 to the plasma membrane at the site of bacterial entry. *Nat. Immunol.* **11**, 55–62.
- Unterholzner, L., Keating, S.E., Baran, M., Horan, K.A., Jensen, S.B., Sharma, S., Sirois, C.M., Jin, T., Latz, E., Xiao, T.S., et al. (2010). IFI16 is an innate immune sensor for intracellular DNA. *Nat. Immunol.* **11**, 997–1004.
- Watson, R.O., Manzanillo, P.S., and Cox, J.S. (2012). Extracellular *M. tuberculosis* DNA targets bacteria for autophagy by activating the host DNA-sensing pathway. *Cell* **150**, 803–815.

Wu, J., Sun, L., Chen, X., Du, F., Shi, H., Chen, C., and Chen, Z.J. (2013). Cyclic GMP-AMP is an endogenous second messenger in innate immune signaling by cytosolic DNA. *Science* 339, 826–830.

Xia, X., Cui, J., Wang, H.Y., Zhu, L., Matsueda, S., Wang, Q., Yang, X., Hong, J., Songyang, Z., Chen, Z.J., and Wang, R.F. (2011). NLRX1 negatively regulates TLR-induced NF- κ B signaling by targeting TRAF6 and IKK. *Immunity* 34, 843–853.

Zaki, M.H., Vogel, P., Malireddi, R.K., Body-Malapel, M., Anand, P.K., Bertin, J., Green, D.R., Lamkanfi, M., and Kanneganti, T.D. (2011). The NOD-like re-

ceptor NLRP12 attenuates colon inflammation and tumorigenesis. *Cancer Cell* 20, 649–660.

Zhang, Z., Yuan, B., Bao, M., Lu, N., Kim, T., and Liu, Y.-J. (2011). The helicase DDX41 senses intracellular DNA mediated by the adaptor STING in dendritic cells. *Nat. Immunol.* 12, 959–965.

Zhong, B., Yang, Y., Li, S., Wang, Y.Y., Li, Y., Diao, F., Lei, C., He, X., Zhang, L., Tien, P., and Shu, H.B. (2008). The adaptor protein MITA links virus-sensing receptors to IRF3 transcription factor activation. *Immunity* 29, 538–550.